Integrating UAS Swarming with Formation Drag Reduction

John Colombi, David R Jacques, Jacob L. Lambach
Department of Systems Engineering and Management
Air Force Institute of Technology (AFIT)
Wright-Patterson AFB OH USA
john.colombi@afit.edu

Abstract— **In the seminal research into simulated swarming, Reynolds developed a methodology that guided a flock of agents using just three rules: collision avoidance, swarm centering, and velocity matching. By modifying these rules, an algorithm is created and applied to unmanned aircraft systems (UAS) so each aircraft in a "swarm" maintains a precise position relative to the preceding aircraft. Each aircraft experiences a decrease in induced aerodynamic drag, thus reducing overall fuel consumption, increasing range and endurance and expanding UAS utility. A simulation demonstrates the feasibility of the drag reduction swarm using a drag benefit map constructed from extant research. Due to both agent interaction and wind gust variability, the optimal position for drag reduction presented a severe collision hazard, and drag reduction was much more sensitive to lateral (wingtip) position than longitudinal (stream-wise) position. By increasing longitudinal spacing, the collision hazard was acceptably reduced. For one scenario, compared to a single UAS, a swarm of 10 aircraft demonstrated a 9.7% reduction in total aerodynamic drag, decreased fuel consumption by 14.2% and an increased endurance by 14.5%.**

Keywords— Autonomous agents, Adaptive control, Multi-agent systems, Cooperative systems, Unmanned aerial vehicles, Simulation

I. INTRODUCTION

Over the last several years, operations by the United States military have demonstrated the growing importance of Unmanned Aircraft Systems (UAS). There is now a vastly growing UAS market for many commercial applications, including agriculture, imagery, real estate, sports photography, and shipping/commerce. As UAS operations and technology grows in prominence, there exist opportunities for new roles such as swarming. Blending concepts from Clough [1] and the US Air Force UAS Flight Plan [2], a swarm is "a collection of autonomous agents relying on local sensing and local implemented behaviors, interacting toward a focused mission goal." Swarming offers new capabilities such as increased payload, greater area coverage, and lower pilot/operator workloads. Additionally, there may be opportunities, especially for dangerous applications, to accomplish the same mission as conventional manned aircraft by substituting a fuel-efficient swarm [3] [4].

While significant research has been undertaken into swarming algorithms, one additional benefit of swarming that has not been fully documented is the increased efficiency of swarming [5] [6]. Past research has examined the increased efficiency gained by taking advantage of wake vortices from previous aircraft [7] [8], but that work has not been integrated with more than two aircraft.

Studies assert that utilizing wake vortices can reduce induced drag by up to 54%, resulting in greatly decreased fuel consumption and increased range and endurance [9]. However, the proximity and coordination required to yield significant drag reduction benefits are significantly more complex than that of existing swarming models. As such, swarming models and formation drag reduction have been, up to this point, mutually exclusive. This paper integrates these two concepts (swarming algorithms with formation drag reduction) to take advantage of the benefits of both.

The research uses a simulation constructed using MATLAB. In this simulation, a virtual swarm navigates through a set of waypoints while attempting to maintain the appropriate formation position so that each aircraft may benefit from the preceding aircraft's wake vortices. It uses aerodynamic benefit maps developed in extant research and determines the fraction of time each individual aircraft is able to reap these benefits. Then, fuel consumption, range, and endurance can be calculated empirically. Different variations of the control methodology were tested to determine which factors were significant in increasing swarm range and endurance. This paper specifically addresses: 1) how the formation affects aerodynamic properties of the individual aircraft, such as optimum cruise speed, 2) the formation position that provides the optimum combination of drag reduction and collision avoidance, and 3) the descriptive parameters, control mechanisms and procedures of the formation that drive increased utility..

II. BACKGROUND

A. Swarming and Formations

The United States Air Force utilizes formation flying for a multitude of motivations, both for fighters and larger mobility aircraft [10], [11]**.** The motivation for the swarming behavior displayed by many species of birds is a source of debate in the biological community. Many point to aerodynamic benefits of flying in a formation. Other theories include mutual defense against predators, ease of communication, and social behaviors, which are similar to the motivations listed for

978-1-5090-4623-2/17/$31.00 ©2017 IEEE

fighter aircraft [12], [13]. Research suggests that the former theory (aerodynamics) is more applicable to larger birds while the latter theories are more appropriate for smaller birds [14].

In order to implement a semi-autonomous swarm of agents, most algorithms employ a variety of "rules" which are weighted in order to adjust changes to each agent's velocity. Craig Reynolds originated this concept with three simple behavioral rules: collision avoidance, velocity matching, and swarm centering. Collision avoidance implies the urge to move away from the closest swarm members. Velocity matching seeks to match both speed and direction of travel with the rest of the swarm. Finally, swarm centering urges each bird to move toward the center of the swarm, to maintain the benefits of the swarm. Reynolds later introduced other potential behavioral rules: a migratory urge that causes the entire swarm to move in a specified direction and a desire to avoid environmental obstacles [6].

While Reynolds refers to his grouping as a "swarm", his rules tend to produce a cluster rather than an ordered formation. Nathan and Barbosa [13] modified Reynolds's rules to attempt to form a V-like formation like those found in nature. They orient each simulated bird so that it had an unobstructed longitudinal view. Their birds would first seek to establish proximity to birds within a specified radius. Next, they would move relative to the neighbor in order to obtain an unobstructed view. Finally, the birds would move to maintain a specified station relative to the others.

Many other theories, rules, and weighting schemes exist, but the swarming theories all tend to feature various sets of rules, which govern acceptable behavior for the individual agents within the swarm, and various techniques for judging which rule is most important for any moment in time [16] [17]. While algorithms vary, it will be shown that significant benefit can be gained from using an algorithm that forms the swarm into a "V" formation.

B. Formation Drag Reduction

While other methods of improving energy efficiency in aircraft design and operations exist, increasing efficiency through formation flight is still in relative infancy. A concept is borrowed from migrating geese that fly in a "V" formation to reduce overall workload. In aerodynamic terms, the wings of each bird (or aircraft) produce vortices because of the pressure differential across the top and bottom wing. This wake turbulence vortex trails behind the aircraft and creates an upwash outboard of the wingtips and a downwash inboard of the wingtips [17]. By positioning a trailing aircraft within the upwash from the previous aircraft, the lift vector of the trailing aircraft is rotated so that lift is marginally increased and induced drag is substantially reduced. While there are other forms of drag, under normal circumstances induced drag comprises approximately 45% of total drag [18]. Any drag reduction will likely lead to an increase in fuel efficiency.

Formation drag reduction originated in the field of biology. In 1970, Lissaman and Shollenberger [19] calculated that a swarm of 25 birds could theoretically achieve a range increase of 71 percent over a lone bird, or more with a tailwind. Additionally, they asserted that the lead bird (tip of the "V") did not actually have the highest workload as long as the "V" had two legs because it could experience the upwash from the birds trailing it. They observe, "the optimal shape of the V formation, while swept, is not an exact V; it is more swept at the tip and less at the apex."

Hainsworth [20] expanded upon this research in 1986 by observing actual swarms and comparing their formations with those theoretically proposed by Lissaman and Shollenberger. He showed that most birds trailed one to three wing spans behind the bird ahead of them, though the gap between the lead and second bird was actually wider than subsequent ones, in direct contradiction to Lissaman and Shollenberger's optimal formation. Additionally, he shows that in practice, geese achieve a 36% reduction in induced drag; about half of the theoretical maximum, but the geese demonstrate active corrections toward the optimum position.

Drag reduction efforts are primarily divided into two categories: close and extended formation. Close Formation (CF) implies that the streamwise separation between aircraft is very small, in the magnitude of 0-5 wingspans, and is primarily useful for UASs and fighter aircraft. Extended Formation (EF) targets 15-40 wingspan streamwise separation and is more useful for larger mobility and commercial aircraft. Computational fluid dynamics indicate that most fuel savings can be maintained even when the following distance is increased to 15-40 wingspans, yielding an induced drag reduction of 54% at subsonic airspeeds. At the optimal location where 90% of energy benefits can be achieved, variations of 5% of the wingspan in vertical and 10% in lateral are allowed. However, only the trail aircraft experiences drag reduction in EF, as opposed to both aircraft in CF [9].

Close Formation (CF) presents the potential for greatest drag reduction, but also presents additional challenges due to the increased risk of mid-air collision. NASA's Dryden Flight Research Center has conducted extensive research into close formation flight using F/A-18s for data collection. In 1998, they demonstrated a 10-15% reduction in drag when flying within the vortex [21]. They built upon this research by implementing autonomous control techniques to maintain close formation positioning - within 10 cm. NASA was able to demonstrate via flight test that formation flight provides induced drag reduction similar to theoretical models [5].

These reductions in induced drag led to demonstrated reductions in overall drag of 20% and reductions in fuel flow of 18%. This study also found that maximum benefit was obtained at the positions shown in Table 1. Values are calibrated to the airplane wingspan b and referenced so that (0,0,0) indicates aircraft completely overlapping, while decreasing values of X, Y, and Z indicate moving aft, inboard, and down respectively [8]. This study showed the benefit region maintained a predictable location with longitudinal separations up to 5 wingspans, but began to wander slightly at further aft positions. In 2002, Wagner performed a similar flight test and showed 8.8% ± 5.0% fuel savings when flying two T-38 aircraft in close formation [7].

TABLE I

Region of Peak Drag Reduction Benefit

	Longitudinal wingspan (X)	Lateral wingspan (Y)	Vertical wingspan (Z)
Lower Bound	-3.0	0.80	-0.10
Upper Bound	-4.4	0.90	0.0

For a group of small UASs, the close formation position seems to be more appropriate. The tradeoff between the greater drag reduction of close formation (Fig 1) and the simplified collision avoidance of the extended formation introduces an imperative to find an acceptable compromise. Although controllers have been developed that maintain close formation with two aircraft [22], the uncertainty lies in developing a guidance system that will enable a formation larger than two aircraft, while simultaneously reacting to varying atmospheric conditions and mission requirements, as well as dynamic local behaviors across the formation.

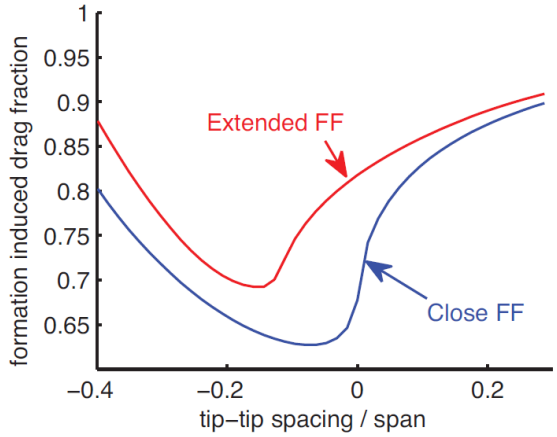

Fig 1. Close vs. Extended Formation Flight (FF) [19]

C. *Guidance Mechanisms*

Techniques have been proposed for controlling a large formation of aircraft with precise station-keeping requirements. The most intuitive and basic approach is for each aircraft to simply maintain the desired position relative to its immediate predecessor. The obvious alternative to this approach is for each aircraft to maintain an appropriately scaled position relative to the overall leader of the formation.

Innocenti et al. [4] refer to these various approaches as Front Mode and Leader Mode respectively, as illustrated in Fig 2. They show that Front Mode "presents a poorer transient response, due to error propagation." This phenomenon is known as string instability; the longer the string of followers grows, the more unstable the station-keeping becomes. Seiler et al. [14] show that the Front Mode will be unstable when using any linear control law, but asserts that Leader Mode can still be used because aircraft near the rear are able to anticipate changes and damp out error propagation.

An alternative guidance system is also provided by Innocenti et al. This approach requires each aircraft to maintain a desired position relative to the Formation Geometric Center (FGC), (Fig 2, center X mark). This idea is derived from migratory patterns of swarming birds [4]. This guidance mechanism is easy to adapt to current swarming algorithms, as the Reynolds's rule to move to the swarm center could be replaced with a position relative to the FGC.

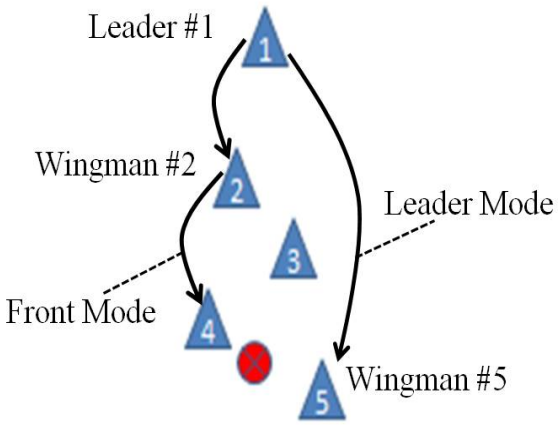

Fig 2. Basic Guidance Control Methodologies

III. Methodology

A. *Control Logic*

A swarming simulation was built using Reynolds's three basic rules as the baseline: collision avoidance, swarm centering, and velocity matching. Each rule was modified for the specific requirements to achieve drag reduction from wake vortices. The biggest change was modifying the swarm centering rule to incorporate positions relative the Formation Geometry Center. This allows the simulated swarm to maintain precise relative positions, even while navigating through turns. Tests were performed on various control parameters to determine which configuration maximized aerodynamic benefits.

In order to experience the aerodynamic benefits from wake vortices, aircraft must maintain precise positions with respect to each other. To accomplish this while promoting overall swarm stability, each aircraft exchange their current position and velocity during each simulated timestep.

1) *Rule 1 – Velocity Matching*

The Velocity Matching rule is simplest and encompasses navigation toward the next waypoint in the swarm's desired flight plan. The output of the rule is designed to accelerate or decelerate each aircraft to an aerodynamically optimum airspeed. Since the overarching purpose of integrating swarming with formation drag reduction is increasing fuel efficiency, it is imperative to motivate the swarm toward an optimum airspeed when not overridden by other concerns. Because velocity includes both speed and direction, this rule also attempts to turn each aircraft toward a desired direction – in this case the direction from the center of the swarm to the next waypoint.

2) *Rule 2 – Swarm Centering*

The Swarm Centering rule has been extensively modified from Reynolds's methodology to become a "Station Keeping"

behavior. Each aircraft assigns itself a formation position number according to the numbering convention of Fig 3. The desired spacing between each aircraft is chosen to maximize drag reduction in accordance with Table I. Because the position of maximum benefit actually requires wingtips to overlap, a stagger is introduced to move the aircraft on the right side of the formation aft by half the normal spacing to aid in collision avoidance, as shown in Fig 7b). This is acceptable because drag reduction is much more sensitive to lateral than longitudinal changes [9].

Two other sub-behaviors are incorporated into the Station Keeping rule in order to expedite the join-up process: diminishing lead pursuit and location-dependent action. Rather than point toward the drag reduction point, the aircraft estimates where point's progression. Each aircraft uses the swarm's current speed and desired direction to evaluate an aim point in the future, and then adjusts speed and heading to arrive at that point at the right time. As the aircraft nears the desired position, the forward look-ahead distance decreases.

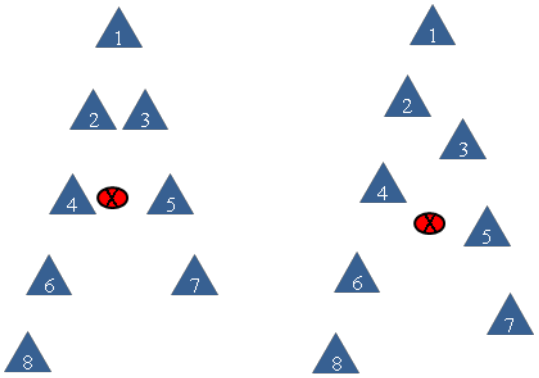

Fig 3. Formation Geometry Center (FGC): a) Aligned Position and b) Staggered Position

The other sub-behavior is a directional location-dependent action. Specifically, the action taken by the aircraft to maneuver to its desired position is dependent on the relative locations of its current and desired position. If the desired position is in the forward (green) region shown in Fig 4, the diminishing lead pursuit algorithm will be used. Conversely, if the desired position is to the back (red) region, the aircraft will simply slow down and wait for the swarm to "catch up."

This sub-behavior is accomplished to prevent drastic overcorrection, maintain a stable flight path, and conserve fuel. For corrections to either side (yellow), the aircraft will slow down and commence a turn toward the desired position, which will quickly move it into the forward (green) region.

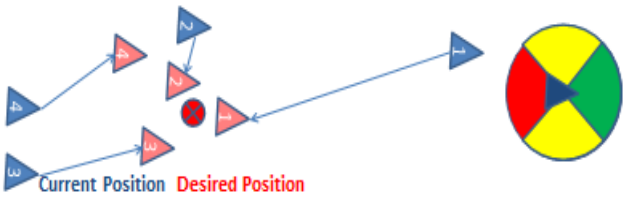

Fig 4. Location-Dependent Action

3) Rule 3 – Collision Avoidance

The third rule, Collision Avoidance, is straightforward. A buffer radius is established. If any aircraft are within a circular region defined by buffer radius, current velocities are compared to see if separation distance is increasing or decreasing. If decreasing, an immediate evasive turn away and acceleration/deceleration is commanded. Additionally, the input is scaled proportional to the inverse of separation distance; the closer the intruder is, the larger magnitude of the evasive behavior. One additional sub-behavior is incorporated in this rule. If any aircraft is rapidly maneuvering with respect to the rest of the formation, the size of the buffer zone is increased so that it begins evasive actions earlier. This is necessary because aircraft with large heading differentials move very rapidly relative to the rest of the formation and therefore close aircraft need to commence evasive actions earlier in order to avoid collisions.

While position changes are normally only initiated after turns, it also makes sense to change positions occasionally during prolonged straight segments. This occurs because the lead aircraft does not reap any aerodynamic benefit with intermediate longitudinal spacing values and will burn its fuel more quickly than the others, if it does not have a chance to move to a different formation position. Alternatively, one aircraft could be designated as the "permanent lead" and maintain the #1 lead position at all times, especially if this aircraft is configured to carry additional fuel.

4) Rule 4 – Formation position changes

A fourth function is incorporated at the same time that the other three rules are calculated. At every time step, each aircraft determines if it should maintain its current formation position or move to a different position. Formation position changes are normally initiated after turns (waypoints) in order to reform the proper formation in a minimum amount of time. After the swarm geometric center has passed the waypoint, each aircraft calculates an angle between two lines: one going from the swarm center point to itself, and another going from the swarm center point to the next waypoint. Because each aircraft knows the position of the other aircraft in the swarm, it is able to calculate these angles for each of the other aircraft. The aircraft which has the smallest turn angle, determines itself the new "#1" lead aircraft; the aircraft which has the next lowest positive value becomes "#2" and so on. Observations showed that this is only beneficial for turns of large magnitude, over a pre-defined threshold. Else, all aircraft will maintain their current position through the turn.

5) Accumulation of Rules

After the results of rules are calculated, the outputs are accumulated into a weighted average. A damper (low pass filter) is applied for aircraft that are near their desired position to prevent destabilizing small rapid corrections. Next, aerodynamic limitations are applied to each aircraft's proposed turn and acceleration. These limits include:

- Maximum turn rate (based on bank angle and g-limits)
- Roll rate (change in turn rate per unit time)
- Minimum and maximum velocity

- Maximum linear acceleration and deceleration

B. *Aerodynamic Calculations*

The simulation uses specifications for a typical UAS; the Aerosonde, with a 2.9m (9.7 ft) wingspan, is a representative UAS for swarming scenarios. As aircraft advance throughout the simulation, multiple aerodynamic properties are continuously being calculated. A combination of constant settings (air density, wing area) and variable factors (desired acceleration, wingtip vortex effects) are used to determine the fuel consumption value for every time step of the simulation. In this case, typical aerodynamic coefficients such as drag, efficiency and wing surface area (C_{D_0}, ε, and S) are taken from the Aerosonde specifications. It is worth noting that the factors of interest are *relative* fuel savings and drag reduction when multiple UASs fly in an optimum formation. Overall, the actual coefficients themselves are relatively unimportant and results should be scalable to other airframes of the general size and wing shape.

The calculations begin with a Free Body Diagram (Fig 5) and Newton's second law, $F=ma$. Again, as the goal of this paper is to demonstrate relative gains rather than absolute values, some simplifying assumptions are made. Thrust and Drag forces act purely in the horizontal plane and Lift forces act orthogonal to the direction of flight. These assumptions are fairly accurate in level flight with normal angle of attack values. Since the simulation models level flight, there is no vertical acceleration and therefore lift is equal to weight (L-W=0).

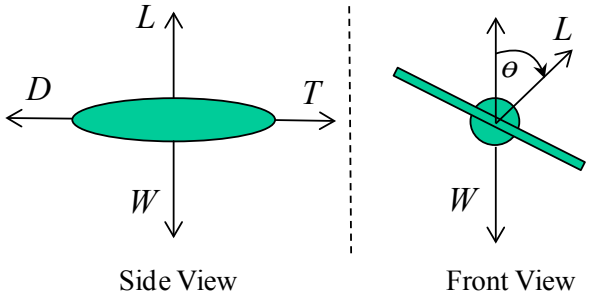

Fig 5. Aerodynamic Forces Free Body Diagram

Start with fundamental lift and weight equations.

$$\left(\frac{1}{2}\rho V^2 S C_L\right)\cos\theta = mg \tag{1}$$

where ρ is *air density*,
V is *velocity*,
S is *planform wing area*,
C_L is the *coefficient of lift*,
θ is *bank angle*,
m is *mass*, and
g is *acceleration due to gravity*.

Because ρ, S, and g are constant throughout the simulation (See Table II), and m, V, and θ are determined in the simulation, Eq 1 can be rearranged to calculate C_L.

$$C_L = \frac{2mg}{\rho V^2 S\cos\theta} \tag{2}$$

Newton's second law is used to calculate horizontal forces:

$$T - \tfrac{1}{2}\rho V^2 S C_D = ma \tag{3}$$

where T is *thrust required*,
C_D is the *coefficient of drag*, and
a is *linear acceleration*.

The drag coefficient is typically split into multiple components: skin friction, form drag, and induced drag. Skin friction drag and form drag are often combined into one term: the zero-lift drag coefficient, C_{D_0}, while induced drag is calculated as a fraction of the square of C_L. However, in this case, the induced drag coefficient has an added term because the wake vortices only affect induced drag. Thus, C_D is calculated as:

$$C_D = C_{D_0} + \left(\frac{C_L^2 S}{\pi b^2 \varepsilon}\right) C_{DR} \tag{4}$$

where b is *wingspan*,
ε is the *efficiency number*, and
C_{DR} is the *coefficient of drag reduction* caused by wake vortices.

Because b, ε, and C_{D_0} are constant throughout the simulation (Table II) and C_{DR}, m, and a are calculated every time step, required thrust (T) can be computed by combining Equations 2, 3, and 4 to form Equation 5:

$$T = ma + \tfrac{1}{2}\rho V^2 S\left[C_{D_0} + \left(\frac{\left(\frac{2mg}{\rho V^2 S\cos\theta}\right)^2 S}{\pi b^2 \varepsilon}\right) C_{DR}\right] \tag{5}$$

Fuel consumption is assumed to be linearly related to thrust produced, although this is not necessarily true at extreme throttle settings. Specifically, a specific fuel consumption value of 0.009286 kilograms/N·hr is derived from actual performance of an Aerosonde as demonstrated by Laima [23]. Fuel consumed is then subtracted from the mass of the aircraft and monitored as the simulation proceeds.

TABLE II. Aerosonde UAV Aerodynamic Coefficients [24]

PARAMETER	VALUE
m (Zero Fuel Mass)	8.5 kg
S (Planform Wing Area)	0.55 m^2
b (Wingspan)	2.8956 m
ρ (Air Density)	1.268 kg/m^3
ε (Efficiency Factor)	0.1592
C_{D_0} (Zero-Lift Drag Coefficient)	0.03
g (Gravity Constant)	9.8 m/s^2

C. *Measures of Performance (MOP)*

In order to assess the effectiveness of the swarm's control methodology, several measures of performance are identified and captured in the simulation, per scenario.

- Average Distance Out of Position – a cumulative average for all aircraft of the difference between actual position and desired position
- Total Number of Hits (#) – the number of times that the distance from the center of one aircraft to the center of any other aircraft was less than the wingspan of the aircraft (2.9m)
- Total Number of Near Misses (#) – the number of times that the distance from the center of one aircraft to the center of any other aircraft was less than double the wingspan of the aircraft (5.8m)
- Cumulative Time in Position– a cumulative average of of time that an aircraft was within 10% of the desired drag-reducing position, both laterally & longitudinally
- Time to Reach Position – the average amount of time that it took for the entire swarm to reform into the commanded formation after each turn/ waypoint.
- Average C_{DR} – A cumulative average of the coefficient of drag reduction experienced by the swarm, excluding the lead aircraft
- Cumulative Fuel Savings– the percentage difference between fuel consumed versus fuel that would have been consumed if the benefits of wake vortices (C_{DR}) had been ignored
- Specific Range (nm/kg) – the total distance traveled by the swarm scaled by the total amount of fuel consumed
- Fuel Consumption Standard Deviation – a measure of the variance across the fuel consumption of all aircraft

IV. Analysis and Results

Using the simulation, the swarm parameters were tuned by applying adjustments to the configuration factors (Table III), such as the sensitivity and magnitude of dampers, the frequency of changes in formation positions, and how often the desired acceleration (time step) is calculated. The tuning process began with a broad screening experiment and moved on to individually adjusting parameters to optimize the measures of performance (MOPs). A delicate balance was required to weigh the competing interests of minimizing collisions and decreasing fuel consumption. Next, two mission scenarios were constructed to analyze how a swarm, which integrates formation drag reduction, increases performance relative to a baseline.

A. *Screening Experiment*

An initial simulation was conducted to determine relationships between various configuration variables and the Measures of Performance (MOPs). The statistical analysis program JMP was used to design a screening experiment using 19 factors (configuration variables) and the 9 MOP response variables. A fractional factorial design was used of order 2^{19-13}, plus a center point, equaling 65 test conditions (2^6+1). Higher order effects were confounded, but main effects and many two-factor interactions were available. Each test condition was replicated 11 times, for 715 runs. Each test run consisted of two hours of simulated flight between randomly generated waypoints. Additionally, random variables were "seeded" across each replicate.

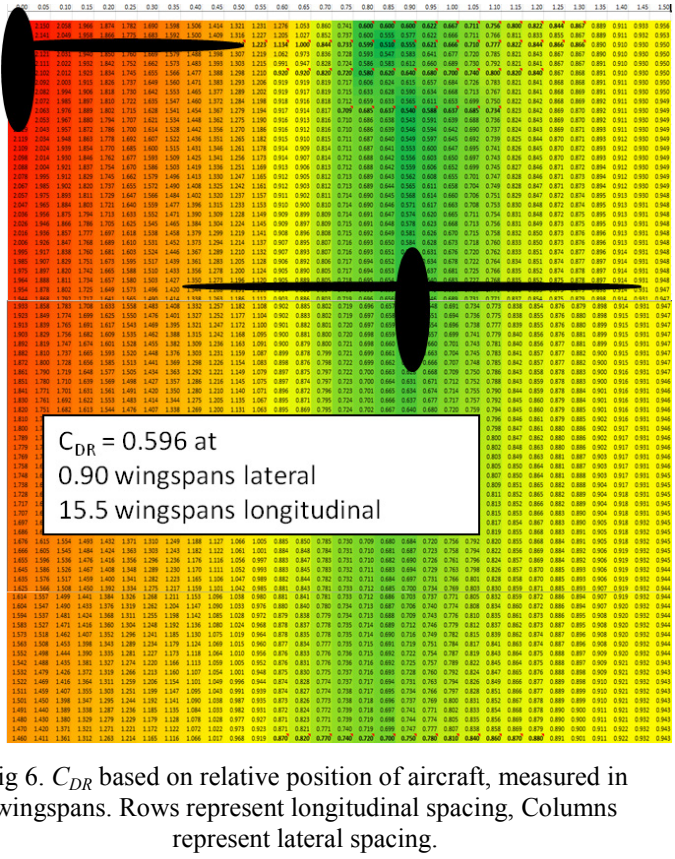

Fig 6. C_{DR} based on relative position of aircraft, measured in wingspans. Rows represent longitudinal spacing, Columns represent lateral spacing.

The screening experiment provides an initial value for parameters and suggests a logical order for iterative parameter selection experiments. Results showed that Longitudinal Spacing had the largest impact on both the number of collisions between aircraft and near misses. Other less significant, but high contract factors were Time Step, Rule 1 and 3 damper parameters, and distance between waypoint turns.

Early trials showed the 7.0 wingspans performed best at minimizing Fuel Consumption Standard Deviation, 5.0 wingspans performed best at minimizing Distance Out of Position, and 6.5 wingspans performed best at maximizing Cumulative Fuel Savings. SAS JMP® was used to fit a second order model to each factor. It was decided to use 6.5 wingspans Longitudinal Spacing for subsequent trials.

For some factors, interaction effects were obvious and could not be ignored. A 3^2 full factorial design was used, with the previously calculated optima as the center test. This allowed interaction effects to be analyzed. This process was repeatedly until optimal values were determined for all configuration parameters, shown in Table III.

TABLE III. RESULTS OF ITERATIVE PARAMETER SELECTION EXPERIMENT

PARAMETER	OPTIMAL VALUE
Cruise Velocity	55 knots
Lateral Spacing	0.9 wingspans
Longitudinal Spacing	6.5 wingspans
Time Step	1.0 seconds
Rotation Interval	240 sec
Reposition Turn Angle	10 degrees
Overall Damper Width	2.0 wingspans
Overall Damper Magnitude	0.45
Separation Margin	0.75
Rule 1 Damper Angle	15 degrees
Rule 1 Damper Magnitude	1.5
Rule 1 Leading Damper	1
Rule 2 Damper Angle	35 degrees
Rule 2 Damper Magnitude	0.30
Rule 3 Damper Angle	30 degrees
Rule 3 Damper Magnitude	0.20
Generation Interval	1.0 sec

B. *Formation Drag Reduction Performance*

After optimizing the factors, a swarm of 10 Aerosonde UASs flying at 55 knots demonstrated an ability to increase performance, even when making frequent 90 degree turns every 0.8 nautical miles. For turns spaced at intervals less than this, trailing aircraft will spend more time in the downdraft from preceding aircraft, decreasing performance. At turns spaced further apart, performance continues to increase steadily until asymptotically approaching a fuel savings of 13-17%, depending on swarm size. One reason that maximum fuel savings increases with swarm size is because the relative contribution of the lead aircraft (which always has a fuel savings of 0%) diminishes as more aircraft are added to the swarm. The minimum turn length, or minimum orbit size, increases as swarm size increases.

These results provide insight into how to better utilize a swarm. If a mission requires the swarm to orbit around a fixed point, approximated by flying a square pattern, then the same drag reduction formation may not be beneficial. Two key operating conditions become evident. The first point occurs where each curve intersects the horizontal axis, at leg lengths between 0.5 and 0.9 miles. For turns more frequent than this, it is more advantageous to split up the swarm. The second crossing point, where large swarms become more beneficial than small swarms, occurs when leg length is greater than ~ 2.5 miles. If a swarm of 15 aircraft were desired to fly a square pattern with side length of 0.7 miles around a fixed point, it would actually be more beneficial to split the swarm into 3 separate swarms of 5 aircraft. This would yield a 2.5% fuel savings rather than a 2.5% fuel penalty, as shown in Fig 7. Therefore, smaller swarms are more beneficial when making frequent turns, with larger swarms becoming more beneficial for longer leg lengths > ~ 2.5 miles.

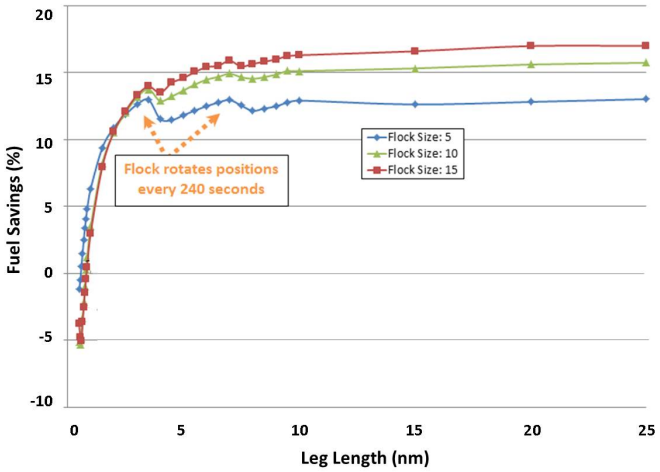

Fig 7. Cumulative Fuel Savings vs. Leg Length Distance (in nautical miles)

C. *Mission Scenario 1*

The simulated swarm conducted two different sample missions; the first is described in this paper. The mission consisted of a long-distance transit to a target area, an extended time orbiting this area, and a return to base. The mission specifies a unique collection of sensors, one carried by each aircraft in the swarm.

The swarm was able to complete the first scenario successfully at airspeeds ranging from 45 to 75 knots, taking an average of 28.4 hrs to accomplish the mission (24 of which were orbiting the target area). Throughout the 597 total hours of simulation time, only one collision was observed. Additionally, the mission profile was accomplished three times. Overall, the swarm experienced a fuel savings of up to 14.2%, depending on cruise airspeed.

Fuel savings is not the only measure of performance, as both the swarming and non-swarming aircraft were able to accomplish the mission; the swarming aircraft simply returned home with more fuel. The true benefit lies in calculating how long the swarm could extend its orbit over the target area. Assuming that the aircraft desired to land with a fuel reserve of 5% fuel capacity, a non-swarming aircraft flying at optimum airspeeds could maintain the target orbit for 31.9 hrs, while the drag reduction formation could maintain the orbit for 36.6 hrs, a 14.5% increase in orbit endurance.

Fuel consumption was compared across three distinct phases of the mission: transit to the target area, orbit over the target, and transit from the target area back to base. Fig 8 highlights an important distinction between best range and best endurance airspeeds. Best range speed is advantageous during transit to and from the target area, whereas best endurance speed is optimal when maintaining an orbit for an extended period of time. It is also worth noting that the best range speed for the swarm of 10 aircraft is approximately 5 knots slower than the best range speed for a single aircraft. This occurs because the wake vortices only affect induced drag, leaving parasite drag unaffected.

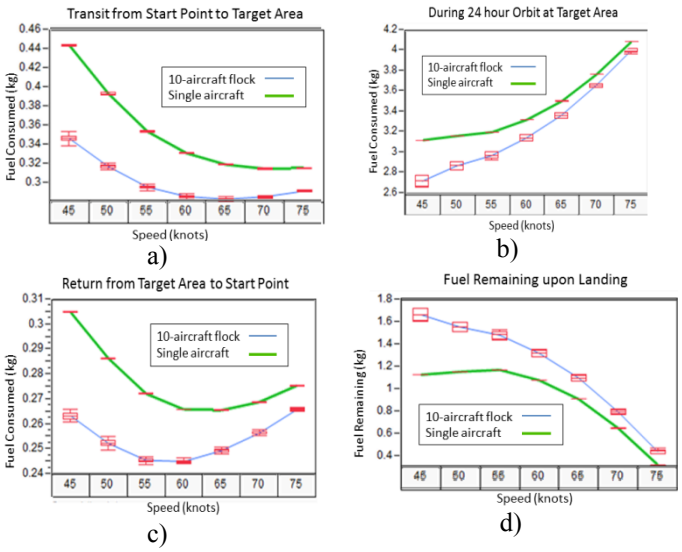

Fig 8. Variability Charts for Fuel Consumption at Different Stages of Mission Scenario One. a) travel to Target, b) orbiting target, c) return travel, d) fuel remaining

The best range airspeed (minimum fuel consumption) is significantly faster at the beginning of the mission than at the end, after mass has decreased due to fuel consumption. This effect also occurs because mass only affects induced drag. With a decrease in mass close to 30%, best range airspeed decreases by about 10 knots for this Aerosonde UAS.

Because the best range airspeed for the swarm is 65 knots and best range for an individual aircraft is 72 knots, one might mistakenly assume that though the swarm is more efficient, the single aircraft can accomplish the mission more quickly. This is inaccurate because the swarm is still more efficient than the single aircraft at all airspeeds. However, the benefit margin decreases as airspeed increases.

V. Summary

The integration of swarming with formation drag reduction has been shown as a realistic concept. The current model provides a feasible compromise between collision avoidance and drag reduction, but provides opportunities to adjust the model if the relative priority of these two objectives changes.

The simulation indicates that the chosen swarming algorithm (modified Reynold's rules) led to a significant decrease in induced drag with corresponding increases in aircraft range and endurance. A minor compromise was required between maximum aerodynamic benefit and collision avoidance. An increase in longitudinal spacing greatly reduced collision potential, while only marginally reducing fuel savings.

The swarm outperformed non-swarming aircraft in all conditions, but by a wider margin when operating at slower airspeeds. Best range airspeeds and best endurance airspeeds were slightly slower for a swarm than for an individual aircraft. Overall, a swarm of 10 aircraft was able to decrease fuel consumption by 14.2% and 14.5% increase in endurance.

VI. References

[1] B. T. Clough, "UAV Swarming? So What are Those Swarms, What are the Implications, and How Do We Handle Them?," in *AUVSI Unmanned System Conference*, Orlando, FL, 2002.

[2] USAF, "United States Air Force Unmanned Aircraft Systems Flight Plan 2009-2047," HQ, United States Air Force, Washington D.C, 2009.

[3] G. Labonté, "Canadian Arctic Sovereignty: Local Intervention by Flocking UAVs," in *IEEE Symposium on Computational Intelligence in Security and Defense Applications*, Ottawa, ON , 2009.

[4] M. Innocenti, F. Giulietti and L. Pollini, "Intelligent Management Control for Unmanned Aircraft Navigation and Formation Keeping," in *NATO Research and Technology Organisation, Applied Vehicle Technology (RTO-AVT)*, Rhode-Saint-Genese, Belgium, 2002.

[5] G. Larson and G. Schkolnik, "Autonomous Formation Flight," NASA Dryden Flight Research Center, Edwards AFB, 2004.

[6] C. W. Reynolds, "Flocks, Herds, and Schools: A Distributed Behavioral Model," in *SIGGRAPH*, 1987.

[7] E. H. Wagner, "An Analytical Study of T-38 Drag Reduction in Tight Formation Flight," Air Force Institute of Technology, WPAFB 2002.

[8] M. J. Vachon, R. J. Ray, K. R. Walsh and K. Ennix, "F/A-18 Performance Benefits Measured During the Autonomous Formation Flight Project," NASA, Edwards AFB, 2003.

[9] J. Kless, M. J. Aftosmis, S. A. Ning and M. Nemec, "Inviscid Analysis of Extended Formation Flight," in *Seventh Int'l Conf on Computation Fluid Dynamics*, Big Island, 2012.

[10] United States Air Force, Air Force Manual 11-251, Volume 1, T-38C Flying Fundamentals, vol. 1, 2011.

[11] North Atlantic Treaty Organization, Allied Tactical Procedures - 56(B): Air to Air Refueling, 2010.

[12] I. L. Bajec and F. H. Heppner, "Organized Flight in Birds," *Animal Behaviour,* pp. 777-789, 78 2009.

[13] A. Nathan and V. C. Barbosa, "V-like Formations in Flocks of Artificial Birds," *Artificial Life,* vol. 14, no. 2, pp. 179-188, 2008.

[14] P. Seiler, A. Pant and K. Hedrick, "Analysis of Bird Formations," in *Proc of the 41st IEEE Conf on Decision & Control*, Las Vegas, 2002.

[15] C. Reynolds, "OperSteer Documentation," 19 Oct 2004. Available: E:\opensteer\opensteer\doc\index.html. [Accessed 28 Jul 2014].

[16] C. W. Reynolds, "Steering Behaviors For Autonomous Characters," in *Game Developers Conference*, San Jose, CA, 1999.

[17] F. Cattivelli and A. H. Sayed, "Self-Organization in Bird Flight Formations Using Diffusion Adaptation," in *3rd IEEE Int'l Workshop on Computational Advances in Multi-Sensor Adaptive Processing*, 2009.

[18] S. A. Ning, "Aircraft Drag Reduction Through Extended Formation Flight," Standford University, 2011.

[19] P. B. S. Lissaman and C. A. Shollenberger, "Formation Flight of Birds," *Science,* vol. 168, no. 3934, pp. 1003-1005, 1970.

[20] F. R. Hainsworth, "Precision and Dynamicsof Positioning by Canada Geese Flying in Formation," *Journal of Exp. Biology,* pp. 445-462, 1987.

[21] National Aeronautics and Space Administration, "1998 Research Engineering Annual Report," NASA, Edwards AFB, 1999.

[22] S. M. Ross, "Formation Flight Control for Aerial Refueling," Air Force Institute of Technology, Wright-Patterson Air Force Base, OH, 2006.

[23] T. McGeer, "Laima: The First Atlantic Crossing by Unmanned Aircraft," The Insitu Group, Bingen, 1999.

[24] R. W. Beard and T. W. McLain, Small Unmanned Aircraft: Theory and Practice, Princeton: Princeton University Press, 2012.